Ivan Bernal, Roger A. Lalancette*, Ahmad Hudaihed and Pavel Kucheryavy

The crystal and molecular structure of (*R*)-sirtinol – $C_{26}H_{22}N_2O_2$ – a chemo-sensitive enhancer and ligand in metal complexes with important bio-inorganic applications

https://doi.org/10.1515/zkri-2024-0073
Received March 24, 2024; accepted May 19, 2024;
published online July 24, 2024

Abstract: Sirtinol is a known inhibitor of sirtuin proteins – a family of deacetylases involved in the physiology of aging. Its crystalline structure has never been determined except when bound to Fe(III) where it participates in the seven-fold coordination of the metal or to Cu(II) where it acts as a bidentate or tridentate ligand. Herein, we describe the structure of this important molecule, as follows: (a) the prevalent form of the keto-enol tautomerism in the solid state, and (b) in solution. Do they match? If not, how? The crystals of (*R*)-sirtinol are characterized by a large number of π–π bonded interactions linking molecules in infinite ribbons, which, in turn, are linked by additional π–π interactions of a variety of types, and by hydrogen bonds. In the latter case, we confirm by NMR that the X-ray determined position of an important H atom is on a N atom rather than on an O, which is how the molecule is usually depicted.

Keywords: sirtinol; tumor growth inhibitors; tautomeric forms; π–π bonds; hydrogen bonds; physiology of aging

***Corresponding author: Roger A. Lalancette**, Carl A. Olson Memorial Laboratories, Department of Chemistry, Rutgers University, 73 Warren St., Newark, NJ, USA, E-mail: roger.lalancette@gmail.com. https://orcid.org/0000-0002-3470-532X
Ivan Bernal, Carl A. Olson Memorial Laboratories, Department of Chemistry, Rutgers University, 73 Warren St., Newark, NJ, USA; and Molecular Sciences Institute, School of Chemistry, University of the Witwatersrand, Private Bag 3, 2050 Johannesburg, ZA, USA, E-mail: bernalibg@gmail.com. https://orcid.org/0000-0002-8168-5907
Ahmad Hudaihed and Pavel Kucheryavy, Carl A. Olson Memorial Laboratories, Department of Chemistry, Rutgers University, 73 Warren St., Newark, NJ, USA, E-mail: ah1238@scarletmail.rutgers.edu (A. Hudaihed), pvk10@newark.rutgers.edu (P. Kucheryavy). https://orcid.org/0009-0009-8356-2327 (A. Hudaihed). https://orcid.org/0000-0003-2286-1779 (P. Kucheryavy)

1 Introduction

In humans, sirtinol arrests the growth of MCF-7 and H1299 cells and inhibits the growth of PC3, DU145, and HeLa cells by enhancing their chemosensitivity to cis-platin. It is also known to markedly inhibit the propagation of adult T-cell leukemia-lymphoma. And, not last of its beneficial properties is its use in the pathophysiology of aging. The literature on sirtinol and related species is vast; therefore, it is notable that the structure of the parent molecule, sirtinol, is not reported in the Cambridge Structural Database[1] either in chiral form or as a racemate. There are in fact a very large number of close relatives in that compilation,[1] but the parent molecule is probably absent because of the difficulty in obtaining high quality crystals of useful size (for details, see below). We are indebted to those colleagues[2] as the source of our sample of pure chiral (*R*)-sirtinol, which is very expensive to get in pure enantiomeric form. Figure 1 is an ORTEP diagram of (*R*)-sirtinol, $C_{26}H_{22}N_2O_2$, with the atoms plotted at the 40 % displacement level.

The structure of bis(nitrato)-(2-(((2-(oxy)-1-naphthyl)methylene)amino)-N-(1-phenylethyl)benzamidato)-iron(III) tetrahydrofuran solvate (HUDNEB), $C_{26}H_{21}FeN_4O_8$ 1.5 (C_4H_8O), has been studied in considerable detail,[2] and the interested reader is encouraged to read that report to acquire information on the properties and physiological characteristics of metal derivatives of sirtinol. Another interesting use of sirtinol is in the form of the Cu(II) derivative; it is bis(1-(((2-((1-phenylethyl)carbamoyl)phenyl)imino)-methyl)-naphthalen-2-olato)-copper(II) benzene acetonitrile solvate, appearing in CSD as TAGCAI in which sirtinol acts, interestingly, in two ways: (a) as a bidentate ligand and (b) as a tridentate ligand, illustrating the versatility of this substance as a metal binding agent.[3] No doubt this versatility influences the ability of sirtinol to interact with biological substrates. This study documents that "assays in cultured breast cancer cells reveal that Cu^{II}(sirtinol–*H*)$_2$ and previously reported Fe^{III}(sirtinol–*H*)$(NO_3)_2$ present enhanced cytotoxicity when compared to the free ligand, and that the ferric complex causes an increase in intracellular oxidative stress." Sirtuin

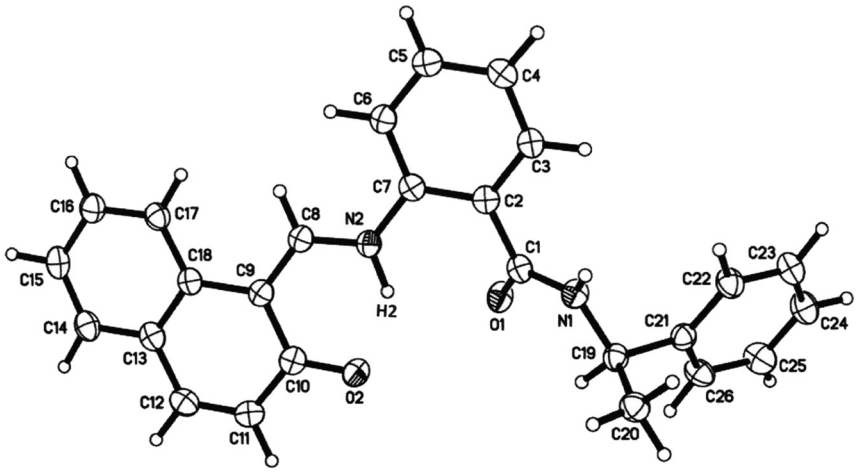

Figure 1: ORTEP representation of the structure of the (*R*)-sirtinol molecule. Atoms are shown at the 40 % displacement level. Note the location of H2 on N2.

proteins are nicotinamide adenine dinucleotide (NAD+)-dependent deacetylases present in mammalian cells in seven isoforms (SIRT1-7).[4] Because of their role in histone modification and gene regulation, the study of sirtuins is relevant to the understanding (at a molecular level) of aging and age-related diseases such as neurodegenerative disorders, diabetes, and cancer.[5,6] These implications have placed sirtuins at the center of intense investigation in the pharmaceutical arena in recent years.

One of the interesting features of sirtinol and related species is the existence of these molecules in either of two tautomeric forms, identified by the position of a proton on the naphthyl ring oxygen or on the external nitrogen. This is a topic of great importance in the chemistry and biochemistry of sirtinol and relatives since in the case of Schiff base reactions (here, we quote directly) "prove that this simple and well-known reaction does not always lead to the obtaining of typical products. In addition, we present a discussion on tautomeric forms preferred by the investigated o-hydroxy imine compounds in solution and in the solid state. Knowledge of the tautomeric form which given Schiff base exists in the solution and in the solid state is very important in the development of medicine and pharmacy…".[7] Further, we note that proton tautomerism can give "rise to excited state tautomers by intramolecular proton transfer enjoy applications as laser dyes, in higher energy radiation detectors, and molecular memory storage devices, as fluorescent probes, and also as polymer protecting agents".[8]

Below, we describe the structural details of the (*R*)-sirtinol molecule itself obtained from more than one solvent and different environment conditions, since their provenance strongly influences the size and quality of the crystals produced. The resulting report below is that of the molecule whose structural information was collected at 100 K and 296 K. For comparison with the X-ray results, NMR studies in $CDCl_3$ gave the location of the proton of interest since no exchange of this proton is observed. Note that it is of major importance to establish whether or not the position of this hydrogen is subject to changes due to changes in the medium wherein the molecule is located; e.g., is there an observable difference between the solid state species (X-ray measurements at 100 K and 296 K) and that in deuterated chloroform at −90 °C?

2 Experimental section

2.1 Crystal growth

Crystals were grown by two different methods: (1) (*R*)-sirtinol was dissolved in THF, and the yellow crystals formed were very long, extremely thin needles, leading to the structure, but not a very impressive one (*R*-factor = 8.1 %); (2) (*R*)-sirtinol was dissolved in THF, on top of which was layered a mixture of THF and hexane, on top of which was layered pure hexane. After 2 days, beautiful thick blocks of yellow crystals formed in the initial THF layer; these are the crystals which we studied at both 100 K and 296 K.

2.1.1 X-ray diffraction

Data for (*R*)-sirtinol, $C_{26}H_{22}N_2O_2$, (I), were collected at 100 K on a Rigaku XtaLAB Synergy-S Dual Source diffractometer equipped with a PhotonJet Cu-microfocus source (λ = 1.54178 Å) and a HyPix-6000HE detector. Data reduction was performed with CrysAlisPro 65;[9] subsequent data processing was also performed in CrysAlisPro. Using the SCALE3 ABSPACK scaling algorithm 66, empirical absorption corrections were applied to the data. Empirical and numerical (Gaussian) absorption corrections, determined by face-indexing and integration, were applied to the data.[10] The

Table 1: Crystal data and structure refinement details for (*R*)-sirtinol.

Chemical formula	$C_{26}H_{22}N_2O_2$
Formula weight	394.46
Temperature/K	100
Crystal system	Orthorhombic
Space group	$P2_12_12_1$
a, *b*, *c* (Å)	5.15508(13), 16.1805(4), 23.8932(4)
Volume (Å^3)	1992.98(8)
Z	4
ρ_{calc} (g cm^{-3})	1.315
μ (mm^{-1})	0.663
F(000)	832
Crystal size (mm^3)	0.107 × 0.067 × 0.043
Θ range (°)	3.30–76.50
Reflections collected	25146
Independent reflections	3927[R_{int} = 0.0821, R_{sigma} = 0.0501]
Reflections observed [$I \geq 2\sigma(I)$]	3265
Data/restraints/parameters	3927/0/337
GOOF on F^2	1.03
Final *R* indexes [$I \geq 2$ (I)]	R_1 = 0.0418, wR_2 = 0.0951
Final *R* indexes [all data]	R_1 = 0.0554, wR_2 = 0.1039
$\Delta\rho_{max}$, $\Delta\rho_{min}$ (e Å^{-3})	0.164, −0.213
Flack parameter	0.0(2)
CCDC no.	2304147

structure was solved by applying the intrinsic phasing in SHELXT and refined by full-matrix least-squares techniques against F^2 (SHELXL) in the OLEX2 graphical user interface.[10] Anisotropic displacement factors were applied for all atoms except for the hydrogen atoms. H atoms were placed in idealized positions and refined using a riding model, except for H2 on N2.[11,12] The positional parameters of this H atom were refined. The crystal data, intensity data collection and structure refinement details are summarized in Table 1. X-ray data for (I) have been deposited in CCDC #2304147. Data were also collected at 296 K, and these data have been deposited with CCDC #2333547. At this point, we must comment that even though the structure remains the same, the displacement parameters of the phenyl group increase markedly at higher temperature, with the consequence that the *R*-factor increases from 4.18 % at 100 K to 5.81 % at 296 K. All of the following discussions are based on the parameters from the 100 K data.

2.2 NMR experimental

All NMR experiments were collected on a Bruker Avance III HD 500 MHz spectrometer equipped with a H/F-BBO probe and an AirJet XR VT unit, and a Varian Inova 600 MHz spectrometer equipped with a broadband HX-5 probe. NMR signals were assigned with ^{1}H, ^{13}C, COSY, HSQC, HMBC, and NOESY at room temperature. For data analysis, Mnova 14.2.1 and Topspin 4.1.3 software packages were used.

^{1}H NMR (600 MHz, $CDCl_3$) δ 14.22 (s, 1H), 9.36 (s, 1H), 8.11 (d, J = 8.4 Hz, 1H), 7.91 (dd, J = 7.8, 1.6 Hz, 1H), 7.89 (d, J = 9.0 Hz, 1H), 7.78 (dd, J = 7.9, 1.3 Hz, 1H), 7.54 (qd, J = 7.2, 1.5 Hz, 2H), 7.39 (ddd, J = 8.0, 6.9, 1.0 Hz, 1H), 7.34 (td, J = 7.6, 1.1 Hz, 1H), 7.32 – 7.27 (m, 2H), 7.21 (dd, J = 7.9, 1.1 Hz, 1H), 7.16 – 7.07 (m, 2H), 6.75 (d, J = 7.6 Hz, 1H), 5.30 (d, J = 7.0 Hz, 1H), 1.54 (d, J = 6.9 Hz, 3H).

^{13}C NMR (151 MHz, $CDCl_3$) δ 165.92, 165.87, 159.55, 146.46, 143.12, 136.70, 133.12, 132.09, 130.11, 129.53, 128.89, 128.72, 128.58, 128.43, 127.93, 127.42, 126.60, 126.33, 126.26, 124.05, 120.80, 120.28, 119.46, 109.60, 49.93, 31.11, 21.96.

For measurements of interatomic distances, a series of NOESY experiments were performed with different mixing times: 100, 300, 400, 500, 600, 800, and 1,500 ms. NOE signals for these mixing times lie in the linear region. For the conformation of the through-bond correlations, COSY was collected at −90 °C.

3 Results and discussion

3.1 NMR results

The signal at 14.22 ppm was assigned to the hydrogen located between the two oxygens and the nitrogen atom. Location of this atom close to three highly electronegative atoms leads to the shift of NMR signal to a weak field. The non-aromatic proton adjacent to C8 was assigned to the signal at 9.36 ppm, which at room temperature, appears as a singlet. Low temperature experiments led to the shift of corresponding protons signals to 14.72 and 9.30 ppm, respectively (see Figure 2a and b).

While the chemical shift of the signal for the –OH/–NH group (14.22 ppm, Figure 2a) indicates the presence of the –OH group, the low temperature ^{1}H experiment and COSY indicate splitting of the signals at 14.72 and 9.30 ppm with coupling constants approximately 2.9 Hz, and correlation between these signals in COSY. These results indicate that the signal at 14.72 ppm (Figure 2b) corresponds to the –NH nucleus (see Figure 3 for the COSY results).

A series of NOESY experiments were performed with mixing times between 100 and 1,500 ms; the intensities of the NOE signals for C(20)H_3–C(19)H and H(C8)–N(2)H correlations (see Figure 4 below for atom assignments) were used for the measurements of the interatomic distances using the equation:

$$\frac{\eta_{IIS}}{\eta_{IS}} = \frac{r_{IIS}^{-6}}{r_{IS}^{-6}}$$

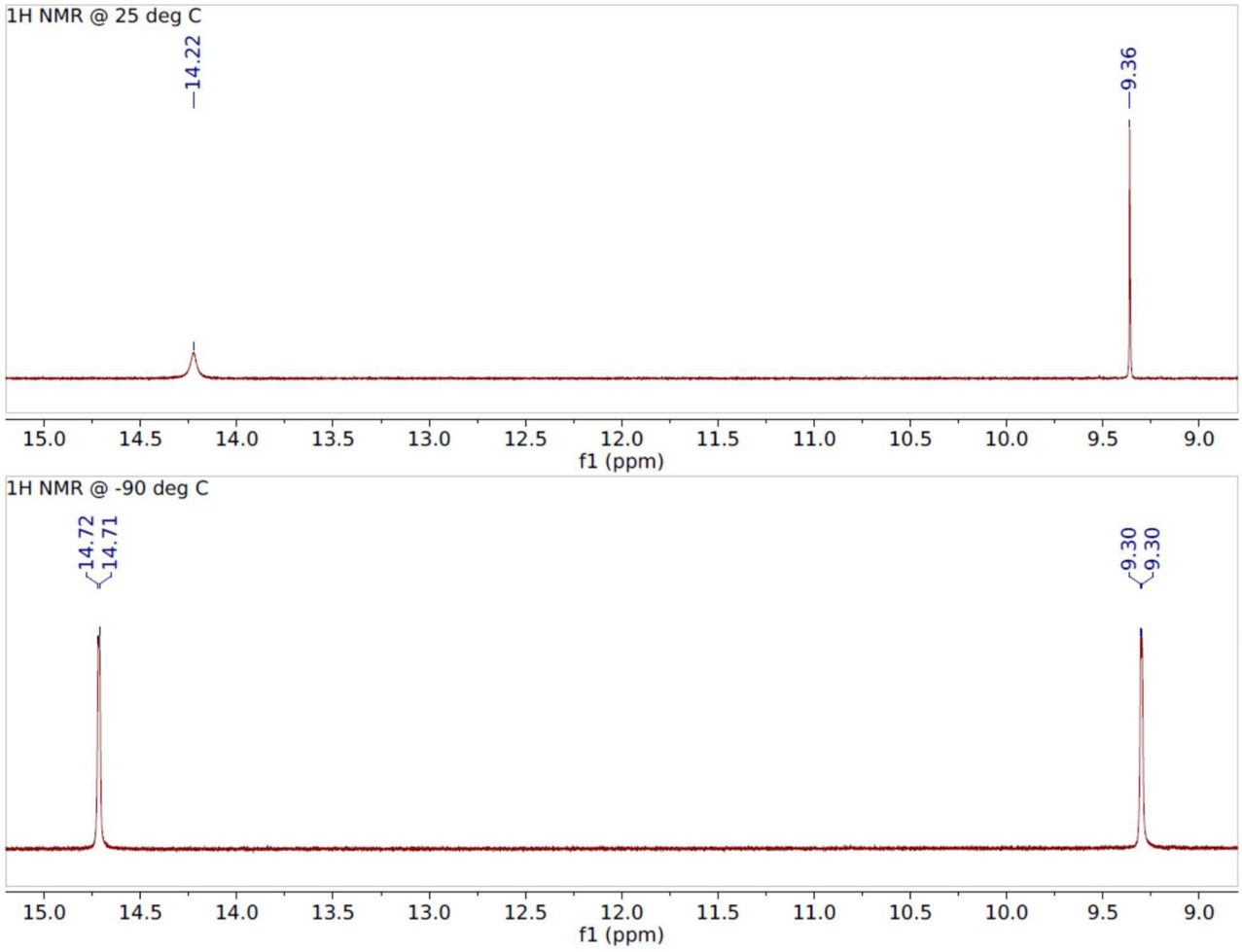

Figure 2: Proton NMR of (*R*)-sirtinol at 25 °C and −90 °C in $CHCl_3$ solution. (a) ^{1}H NMR at 25 °C; (b) ^{1}H NMR at −90 °C.

where η is the intensity of the signal and r is the interatomic distance. If considering r[C(20)H_3–C(19)H] as 2.258 Å [from the common knowledge of the organic molecule's interatomic distances and angles], then the measured H(C8)–NH distance from NOESY experiments is 2.88 ± 0.23 Å (see Figure 4, below). If using crystallographic data, the interatomic H(C8)–N(2)H distance from NOESY is 3.19 ± 0.28 Å. These results are consistent with the observed COSY correlations (see SI for more information).

3.1.1 Conclusion of NMR experiments

Based on the results for NOESY experiments and the low-T ^{1}H as COSY NMR experiments, we can conclude that the ^{1}H signal at 14.72 ppm (see Figure 2b, above) corresponds to the proton found on N2; this correlates directly with what was found by single crystal XRD data [N2–H2 = 1.01(3) Å].

3.2 Results of X-ray diffraction

Below, we display the structure of the molecule in the unit cell of a tautomer of (*R*)-sirtinol crystals grown as described above.

Note that hydrogen H2 belongs to N2 with a distance N2–H2 = 1.01(3) Å; however, the distances to O1 and O2 suggest a trifurcated system with a fairly strong O2···H2 hydrogen bond [1.75(3) Å] and a weaker O1···H2 bond of [2.26(3) Å]. See the NMR results (above) and the Discussion section (below) for the process of locating H2 in this compound. In the X-ray experiment, the distance between H2 and the proton on C8 (namely, H8) is found to be 2.80(5) Å. NMR found this same distance to be 3.19 Å using crystal structural data, and 2.88 Å using commonly known information on distances and angles for organic compounds.

In order to illustrate the fact that such a tautomer is widely documented in CSD,[2] we display below (Figure 5) the structure of one of many such entries present in its current

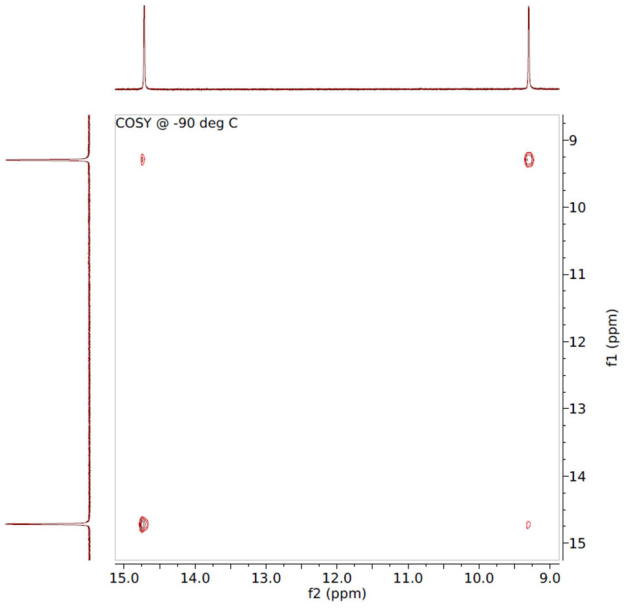

Figure 3: COSY correlation between 14.72 and 9.30 ppm at −90 °C.

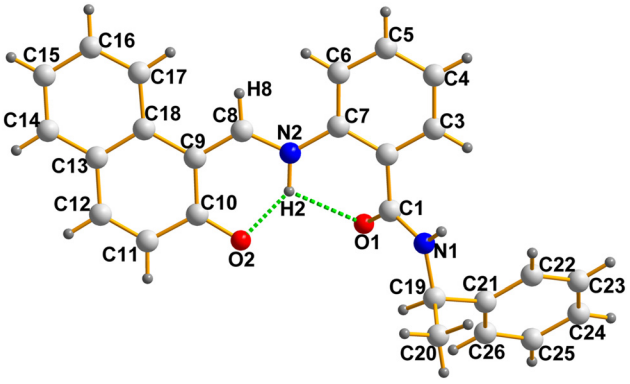

Figure 4: The structure of the (*R*)-sirtinol molecule.

release:[2] entry REMTEK[8] which, despite its distinctly different composition, belongs in the same tautomer class (N–H as opposed to O–H) as that displayed in Figure 4.

Note the nearly exact same N–H distance (N1–H10 = 1.007 Å) observed in this case, despite the difference in composition and conditions upon which the crystals of the two species were obtained (REMTEK[8]). Also the short C9–O1 bond (1.272 Å) is typical of a keto moiety. Table 2 is a comparison of the distances of the "central portion" of (*R*)-sirtinol (I) to REMTEK.[8]

Table 2: Comparison of distances of REMTEK[8] (Figure 5) with the present structure of (*R*)-sirtinol (I).

REMTEK[8] (in Å)[a]		(*R*)-sirtinol (I) (in Å)	
N1–H10	1.01	N2–H2	1.01(3)
N1–C6	1.418	N2–C7	1.414(4)
N1–C7	1.318	N2–C8	1.328(4)
C7–C8	1.402	C8–C9	1.388(4)
C8–C9	1.430	C9–C10	1.454(4)
C9–O1	1.272	C10–O2	1.263(4)
C8–C17	1.429	C9–C18	1.461(4)
H7···H10	2.851	H2···H8	2.80(5)

[a]The uncertainly values for the H atoms in REMTEK[8] are not available from the CIF file for this compound.

Upon displaying the packing of the (*R*)-sirtinol sample, a very notable feature is that the molecules form long ribbons that align very clearly along the *c*-axis of its orthorhombic ($P2_12_12_1$) lattice. Figure 6 displays the packing of the molecules of (*R*)-sirtinol as a *b*-projection that illustrates the effect in question.

In the report by Janiak[13] who analyzed the criteria for meaningful π–π "interactions" between aromatic fragments it was suggested that, given the experimental data then available (see Figure 7 and relevant commentary in that paper), the range of 3.3–3.8 Å is reasonable. Using that as an acceptable gauge, the (*R*)-sirtinol structure displays acceptable "contacts" in that range, as illustrated by the data in Table T2 in the SI. However, we think it is worth pointing out that some meaningful "residual contacts" exist which must contribute to the rigidity of the lattice, particularly in view that such contacts are of a wide variety (see below) and of enormous numbers. Such considerations of limits on meaningful bonds and/or contacts are, of course nothing new, having been debated for years in the discussions of "meaningful" hydrogen bonds. *Caveat Emptor*!

The number of π–π interactions in sirtinol is not only extensive, but of a wide variety of types depending on the nature of the pair components; some of them are shown in Figure 8, below, and tabulated in Table T2 in the SI.

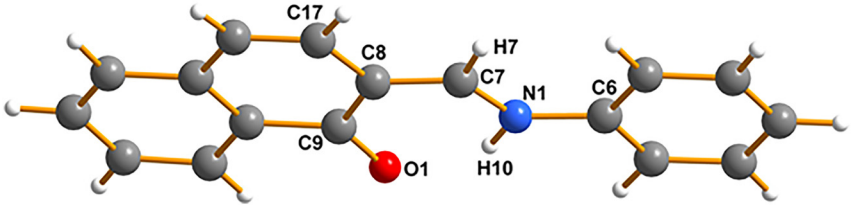

Figure 5: The structure of REMTEK[8] for comparison purposes.

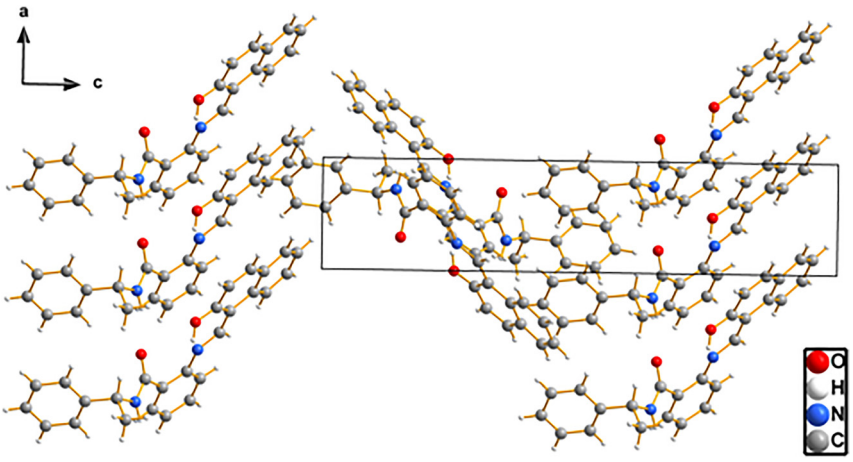

Figure 6: Projection of (*R*)-sirtinol down the *b*-axis, displaying the pronounced, modulated packing of the molecules along the *c*-axis. As shown below, these molecules form continuous ribbons held together by a variety of π–π bonds, as well as some hydrogen bonds, e.g., see Figures 7 and 8, below.

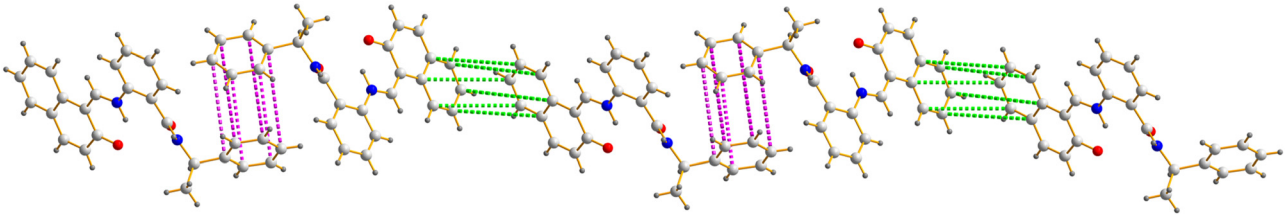

Figure 7: A portion of one of the strings running along the *c*-axis in the crystal of in (*R*)-sirtinol, displaying the alternating modes of π–π bonding contacts that propagate along the entire string, thus lending stability to the infinite ensemble.

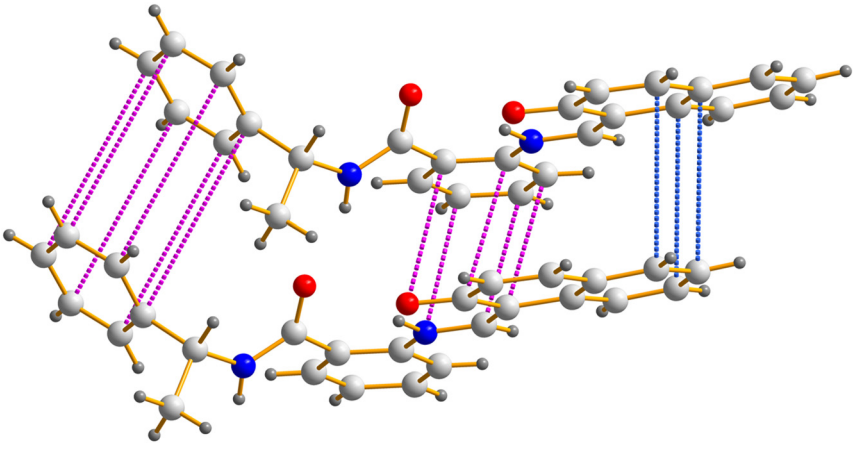

Figure 8: This figure shows multiple different π–π interactions in (*R*)-sirtinol.

Three different π–π interactions in (*R*)-sirtinol are shown: on the left is a weak phenyl-phenyl π–π interaction (one cell apart in a = 5.15508(13) Å); the central and strongest set is between the central phenyl ring and the 6-membered planar ring containing the N–H and the O atoms [values range between 3.526(4) and 3.775(4) Å]; and the right-hand set is between naphthalene-naphthalene rings in adjacent molecules [values range between 4.846(5) and 5.025(4) Å].

Figure 9 shows another set of π–π interactions in (*R*)-sirtinol: this one is between the central phenyl ring (C2–C7) and the naphthalene of an adjacent molecule [1–*x*, *y*, *z*] (see Table T2 in SI). Also shown is a short hydrogen bond between N1–H1···O1 [1–*x*, *y*, *z*] of 2.17(4) Å.

Note the interesting adjacency of phenyl-naphthalene π–π interactions [values range between 4.248 (4) and 4.353 (4) Å]. The complete list of π–π interactions in (*R*)-sirtinol is given in the SI as Table T2.

3.2.1 Conclusions

One of the objects of this exercise was to find out where the proton in (*R*)-sirtinol was located, either on O2 of the

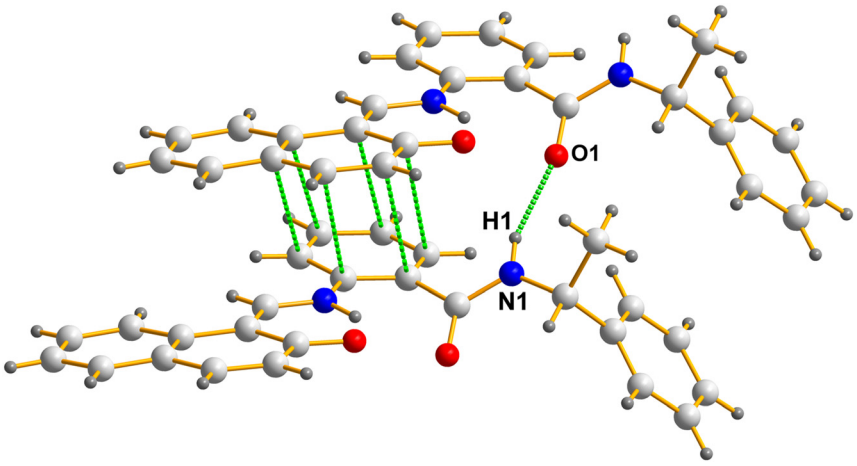

Figure 9: A different type of π–π interactions in (*R*)-sirtinol, as well as intermolecular hydrogen bonds.

naphthalene ring system, or on N2 that is located between the naphthalene and the phenyl ring systems. Because the H2 proton was found on N2 in the crystal structure analysis (see Figure 4), it was imperative that we confirm these results using NMR data. However, this proton also makes close contacts with O1 and with O2 [O1···H2 = 2.25(3); O2···H2 = 1.75(4) A; angles: O2···H2–N2 = 138(3)°; O1···H2–-N2 = 117(2)°; O1···H2···O2 = 103.1(16)°] leading us to believe that this is approaching a trifurcated system.

The X-ray single crystal results definitely show that this proton (H2) is attached to the nitrogen atom (N2), and that in chloroform solution the NMR experiments show beyond any doubt that the proton is bonded to the nitrogen atom (N2). Thus, this feature seems to be a molecular property which is independent of the medium (solid *vs*. solution), as well as the temperature of the sample in the range explored.

Acknowledgments: We thank R. Gautam and E. Tomat for the generous sample of (R)-sirtinol that they sent to us for analysis.
Research ethics: All ethical guidelines have been adhered.
Author contributions: IB and RAL wrote much of the manuscript; PK ran the nmr experiments and wrote that part of the paper; AH crystallized the material and contributed to the structural data, along with RAL. "The authors have accepted responsibility for the entire content of this manuscript and approved its submission."
Competing interests: The authors state no conflict of interest.
Research funding: The X-ray diffractometer used in these studies was purchased with support from the NSF and Rutgers University, grant 2018753.
Data availability: The raw data can be obtained on request from the corresponding author.

References

1. Groom, C. R.; Bruno, I. J.; Lightfoot, M. P.; Ward, S. C. The Cambridge Structural Database. *Acta Crystallogr., Sect. B: Struct. Sci., Cryst. Eng. Mater.* **2016**, *B72*, 171–179.
2. Gautam, R.; Akam, E. A.; Astashkin, A. V.; Loughre, J. J.; Tomat, E. Sirtuin Inhibitor Sirtinol is an Intracellular Iron Chelator. *Chem. Commun.* **2015**, *51*, 5104–5107.
3. Akam, E. A.; Gautam, R.; Tomat, E. Metal-Binding Effects of Sirtuin Inhibitor Sirtinol. *Supramol. Chem.* **2016**, *28*, 108–116.
4. Houtkooper, R. H.; Pirinen, E.; Auwerx, J. Sirtuins as Regulators of Metabolism and Healthspan. *Nat. Rev. Mol. Cell Biol.* **2012**, *13*, 225–238.
5. Roth, M.; Chen, W. Y. Sorting Out Functions of Sirtuins in Cancer. *Oncogene* **2014**, *33*, 1609–1620.
6. Morris, B. J. Seven Sirtuins for Seven Deadly Diseases of Aging. *Free Radical Biol. Med.* **2013**, *56*, 133–171.
7. Mandal, A.; Koll, A.; Filarowski, A.; Mukherjee, S. Intramolecular Hydrogen Bonding in O-Hydroxy Aryl Schiff Bases. *Indian J. Chem., Sect. A: Inorg., Bio-inorg., Phys., Theor. Anal. Chem.* **2002**, *41*, 1107–1111.
8. Nedeltcheva, D.; Kamounah, F. S.; Mirolo, L.; Fromm, K. M.; Antonov, L. Solid State Tautomerism in 2-((Phenylimino)Methyl)Naphthalene-1-Ol. *Dyes Pigm.* **2009**, *83*, 121–126.
9. Rigaku Oxford Diffraction. *CrysAlisPro Software System*; Rigaku Corporation: Oxford, UK, 2019.
10. Dolomanov, O. V.; Bourhis, L. J.; Gildea, R. J.; Howard, J. A. K.; Puschmann, H. J. *Olex2*: A Complete Structure Solution, Refinement and Analysis Program. *Appl. Crystallogr.* **2009**, *42*, 339–341.
11. Sheldrick, G. M. Shelxt – Integrated Space-Group and Crystal-Structure Determination. *Acta Crystallogr., Sect. C: Struct. Chem.* **2015**, *71*, 3–8.
12. Sheldrick, G. M. Crystal Structure Refinement with Shelxl. *Acta Crystallogr., Sect. A: Found. Adv.* **2015**, *71*, 3–8.
13. Janiak, C. A Critical Account on π–π Stacking in Metal Complexes with Aromatic Nitrogen-Containing Ligands. *J. Chem. Soc. Dalton Trans.* **2000**, 3885–3896.

Supplementary Material: This article contains supplementary material (https://doi.org/10.1515/zkri-2024-0073).